Estimating Evaporation in Winter at a Field Irrigated Late in Autumn in Inner Mongolia, China

Kaneko, Takemasa
Graduate School of Bioresource and Bioenvironmental Science, Kyushu University

Kobayashi, Tetsuo
Faculty of Agriculture, Kyushu University

Wang, Weizhen
Cold and Arid Regions Environmental and Engineering Research Institute, CAS

Cho, Hiroyuki
Faculty of Agriculture, Saga University

https://doi.org/10.5109/9262

出版情報：九州大学大学院農学研究院紀要. 51 (2), pp.407-411, 2006-10-27. Faculty of Agriculture, Kyushu University
バージョン：
権利関係：

J. Fac. Agr., Kyushu Univ., **51** (2), 407–411 (2006)

Estimating Evaporation in Winter at a Field Irrigated Late in Autumn in Inner Mongolia, China

Takemasa KANEKO[1]*, Tetuso KOBAYASHI*, Weizhen WANG[2] and Hiroyuki CHO[3]

Laboratory of Applied Meteorology, Division of Regional Environmental Science, Department of Bioproduction and Environmental Sciences, Faculty of Agriculture, Kyushu University, Fukuoka 812–8581, Japan

(*Received June 30, 2006 and accepted July 24, 2006*)

Shortage of water resources has been serious in the Yellow River basin. Therefore, it is expected to reduce the amount of irrigation water without reducing crop production. In the upper reaches, a large amount of water is irrigated late in autumn so that part of the irrigation water remain in a soil profile until next spring and is used for crop germination and development. We evaluated the overwinter water loss due to evaporation at a field irrigated late in autumn, which is a decisive factor for increasing irrigation efficiency. The aerodynamic method, with a dimensionless stability function deduced by Webb (1970), was used to measure the evaporation from a frozen soil surface. Daily evaporation was estimated to range from 0.09 mm to 0.92 mm, which summed up to about 60 mm for the period when the surface soil layer 10 cm thick was frozen (23 November 2004–23 March 2005), which corresponds to about 25% of the amount of irrigation water (Kaneko *et al.*, 2006).

INTRODUCTION

In the upper reaches of the Yellow River, China, wheat, corn (maize), sugar beet, sunflower, cotton, and others are cultivated under irrigation. Annual precipitation in the cultivated areas is less than about 360 mm, and most rainfall occurs in the summer months. Therefore, the discharge of the Yellow River exhibits the seasonal change with a maximum in the mid summer and a minimum in the late spring. Since most crops have to be planted in spring, soil moisture that is essential for their germination is insufficient and is supplied by a method peculiar to this region. After harvest late in autumn, fields are irrigated with a large amount of water diverted from the Yellow River, which is possible because the discharge of the Yellow River is rather large in this season. This region lies at an altitude higher than about 1000 m ASL and is in a latitude of about 40˚N. Therefore, soil moisture near the surface freezes in winter and part of the water supplied by this irrigation is carried over winter as ice in the soil surface layer. However, the authors do not know someone who evaluated the percentage of the irrigation water that remained in the soil surface layer until next spring.

Japan Science and Technology Agency (JST) and Institute of Agro–Environment and Sustainable Development, CAAS, China, established an experimental cornfield at Togtoh in the Yellow River basin (Lat. N 40˚14.8', Lon. E 111˚11.0', Alt. 995 m), Inner Mongolia, China, in order to investigate salinity–controlled, water–saving irrigation techniques. Evaluation of the overwinter loss of the irrigation water due to evaporation is crucial for increasing irrigation efficiency in this region. This paper describes the results of estimating the evaporation from experimental field in midwinter.

OBSERVATIONS

The experimental field, 55×73 m area, is located in an alluvial valley of the Yellow River basin, and basin irrigation is applied with the water diverted from the

Table 1. Climatic characteristics of Togtoh, Inner Mongolia, China. (mean: 1971–2000, extreme: 1971–2002)

Element	Mean / Extreme
Wind speed (mean)	2.3 m s^{-1}
Precipitation (mean)	357 mm yr^{-1}
Precipitation (max)	705 mm yr^{-1}
Precipitation (min)	162 mm yr^{-1}
Air temperature (max)	38.5 ˚C (2 Jul. 2002)
Air temperature (min)	−36.3 ˚C (21 Jan. 1971)
Frozen soil depth (max)	117 cm
Frozen soil depth (min)	87 cm

Table 2. Physical properties of the alluvial soil

Particle size (mm)	% by weight
<0.002	10.3
0.002〜0.075	67.5
0.075〜0.25	17.3
0.25〜0.85	0.2
0.85〜2	4.7
Particle density (g cm^{-3})	2.70
Dry density (g cm^{-3})	1.35
Porosity (−)	0.50
Saturated hydraulic conductivity (cm s^{-1})	1.29×10^{-4}

[1] Laboratory of Applied Meteorology, Division of Regional Environmental Science, Department of Bioproduction and Environmental Sciences, Graduate School of Bioresource and Bioenvironmental Science, Kyushu University

[2] Laboratory of Remote Sensing and GIS, Cold and Arid Regions Environmental and Engineering Research Institute, CAS, China

[3] Laboratory of Geotechnical Environment, Division of Environmental Protection, Department of Environmental Sciences, Faculty of Agriculture, Saga University

* Corresponding author (E–mail: kotetsu@bpes.kyushu–u.ac.jp)

Table 3. Observation system

Variable	Instrument	Height & Depth (m)
Air temperature & Humidity	CAMPBELL, CS500–L6	1.16, 2.52, 3.81, 5.79
Net radiation	CAMPBELL, Q7.1–L20	3.79
Solar radiation	CAMPBELL, LI200X–L11	–
Atmospheric pressure	CAMPBELL, CS105	–
Wind speed	CAMPBELL, 03101–L11	2.50, 3.90, 5.76
Wind speed & direction	CAMPBELL, 03101–L11	7.46
Precipitation	CAMPBELL, CS700–L25	–
Groundwater level	CAMPBELL, CS420–L	–
Ground heat flux	REBS, hft–3.1	−0.05, −0.15
Soil temperature	CAMPBELL, MODEL 107	−0.1, −0.2, −0.4
Soil water content	CAMPBELL, CS615–L50	−0.1, −0.2, −0.4, −0.6, −1.0

river two or three times a year. The climatic characteristics are summarized in Table 1. We can see that frozen soil layers develop to a depth of about 1 m in this area. The soil profile in the experimental field consists of alluvial soil layers, and a thin layer of clayey soil is sandwiched between them at a depth of about 60 cm to 80 cm. The physical properties of the alluvial soil are shown in the Table 2.

Meteorological and hydrological observations were made in the field from the end of April 2003 for three years. Variables and instruments used in this study are summarized in Table 3. Almost all the observations were 10–min averages and taken at intervals of 10 min, though TDR measurements were made on the hour (Beijing Standard Time). The data obtained for the period October 2004 to April 2005 were used in this analysis. Corn was planted at the end of April and harvested on 10 October in this field.

MEASURMENT OF UNFROZEN WATER CONTENT

A frozen soil layer is defined as the layer in which soil moisture is partly frozen. It is almost impossible for the soil moisture to be frozen completely. Volumetric soil water content and unfrozen water content were measured with TDR. It is known that a calibration curve for measuring soil water content in mineral soil can be used for measuring unfrozen water content in frozen soil (Stein *et al.*, 1983). Therefore, the calibration curve for the alluvial soil obtained by Wang *et al.* (2005) was used for measuring the unfrozen water content of soil. It was judged that, when volumetric soil water content at a depth decreased abruptly under freezing winter conditions, frozen soil formed at the depth, and when unfrozen water content increased gradually in early spring and leached a maximum or a peak, the soil thawed completely at the depth. Amount of unfrozen water depends mainly on the soil temperature (Wang and Akae, 2003).

METHODS FOR MEASURING EVAPORATION

Bowen ratio method

The Bowen ratio formula is derived from the energy balance of the bare–soil surface layer, the thickness corresponding to the depth at which G is measured.

$$R_N - G - Lf = H + \lambda E \tag{1}$$

in which R_N: net radiation flux, G: ground heat flux, Lf: heat flux equivalent to fusion (positive) or sublimation (negative), H: sensible heat flux, E: evaporation rate, λ: latent heat of vaporization. Equation (1) can be rewritten in the form

$$\lambda E = \frac{R_N - G - Lf}{1 + \beta} \tag{2}$$

where β is the Bowen ratio ($= H/\lambda E$), which was evaluated by the measurements of air temperature (T) and vapor pressure (e) at two heights using the relation

$$\beta = \gamma \frac{\partial T}{\partial e} \quad \gamma \frac{T_1 - T_2}{e_1 - e_2} \tag{3}$$

where γ is the psychrometric coefficient.

Aerodynamic method

The aerodynamic method relies on the existence of relations between fluxes and gradients

Momentum $\quad \tau = \rho u_*^2 = K_M \partial(\rho u)/\partial z \quad (4)$

Heat $\quad H = -K_H \partial(\rho C_P T)/\partial z \quad (5)$

Water vapour $\quad E = -K_V \partial \rho_V / \partial z \quad (6)$

where, τ, ρ, u_*, u, z, C_P, T, ρ_V, are momentum flux, density of air, friction velocity, wind velocity, height from ground surface, specific heat at constant pressure, air temperature, density of vapor, respectively. K_M, K_H and K_V are turbulent diffusion coefficients for momentum, heat and water vapor, respectively. Since, in neutral stability, $K_M = K_H = K_V$, combination of Equation (5) with Equation (4) yields

$$H = -\rho C_P (\partial T/\partial u) u_*^2 \quad -\rho C_P [(T_1 - T_2)/(u_1 - u_2)] u_*^2 \tag{7}$$

and combination of Equation (6) with Equation (4) yields

$$E = -(\partial\rho_V/\partial u)u_*^2 = -\rho(1-q)(\partial r/\partial u)u_*^2$$
$$-\rho(1-\bar{q})[(r_1-r_2)/(u_1-u_2)]u_*^2 \quad (8)$$

where q is specific humidity, r is mixing ratio and $\bar{q} = (q_1+q_2)/2$.

When a dimensionless stability function ϕ_M is defined as

$$\frac{\partial u}{\partial[\ln(z-d)]} = \frac{u_*}{k}\phi_M \quad (9)$$

Webb (1970) deduced the following relation from the measurements obtained in stable to slightly unstable conditions.

$$\phi_M = [1+5(z-d)/L]^{-1} \quad (10)$$

where L is the Monin–Obukohov length.

$$L = -\rho C_P T u_*^3/kgH = u_* T/kg(\partial T/\partial u) \quad (11)$$

Substituting Equation (10) in Equation (9) and integrating it gives

$$u' = u - 5(z-d-z_0)(\partial T/\partial u)g/T = (u_*/k)\ln[(z-d)/z_0] \quad (12)$$

in which Eq.(11) is used to express L by the measurements taken in this study. Equation (12) can be used to fined $u_*/k = 2.5u_*$ as the slope of the straight line defined by plotting u' against $\ln(z-d)$. When u_* is known, we can get H and E from Equation (7) and Equation (8), respectively (Monteith and Unsworth, 1990).

RESULTS AND DISCUSSION

Weather conditions

Figure 1 shows the seasonal change in daily mean air temperature at a height of 2.52 m and daily precipitation for the period from October 2004 through April 2005 at the Togtoh experimental field. The period from the end of December 2004 through February 2005 had cold temperatures below −10 °C, in which period wind speeds were rather low, though they are not shown in this paper. This suggests that cold temperatures occured when this region was covered with the cold anticyclone.

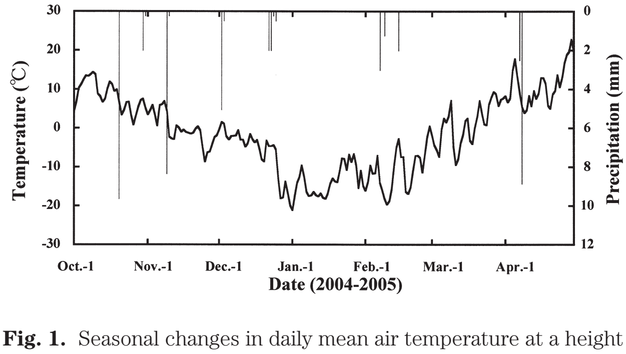

Fig. 1. Seasonal changes in daily mean air temperature at a height of 2.52 m and daily precipitation at the Togtoh experimental field.

Unfrozen water content

Figure 2 shows the seasonal changes in the unfrozen (liquid) water content at depths of 10, 20, 40, 60 and 100 cm at a TDR measurement point and the depth of the water table. Corn was harvested on 10 October and the post–harvest irrigation was applied on 28 October. Daily mean temperature fell below the freezing point in the middle of November. Frozen soils were formed at a depth of 10 cm in the end of November and the freezing front advanced deeper and reached at a depth of 100 cm in the middle of January 2005. A spring thaw at 10 cm started at the end of Feburary and the thaw reached the 100–cm depth in the middle of April.

Seasonal changes in the daily mean soil temperature at depths of 10, 20 and 40 cm in the field are shown in Fig. 3. It is seen that freezing started when the soil temperature fell below zero and thawing started when it rose above zero. It is also obvious that unfrozen water content decreased with increasing soil temperature (Wang and Akae, 2004).

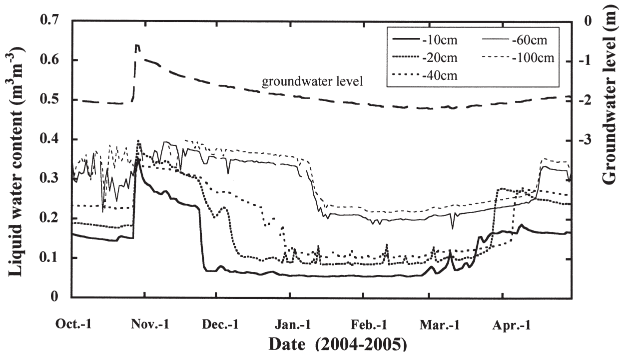

Fig. 2. Seasonal changes in the unfrozen water content at various depths and the depth of the water table.

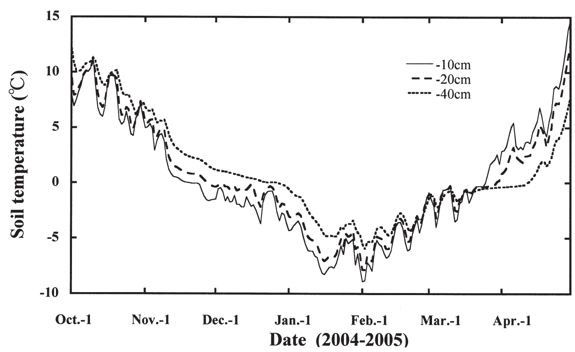

Fig. 3. Seasonal changes in the daily mean soil temperature at depths of 10, 20 and 40 cm.

Evaporation

Temperature and humidity measurements made at heights of 2.52 and 5.79 m, wind speed measurements at heights of 3.90, 5.76 and 7.46 m, and ground heat flux measurements at a depth of 5 cm on the hour were used in the calculation. Since heat of fusion or sublimation in the surface soil layer, Lf, could not be measured, it was assumed that $Lf=0$ when the Bowen ratio method was applied. Furthermore, when the Bowen ratio was within a range of −0.5 and −1.5, measurement of evaporation was resigned at the time and the interpolated value was used when daily evaporation was calculated.

When the aerodynamic method was applied, the wind speed gradient, $\Delta u/\Delta z$, was determined from the regression of u on z using the measurements made at the three heights. When one of the three measurements of u was smaller than $0.5\,\mathrm{m\,s^{-1}}$, the calculation was resigned at the time and the interpolated value was used in the integration to get the daily evaporation, because, otherwise the results showed unstable behavior.

Figure 4 shows the diurnal changes energy balance terms of the bare–soil surface layer 5 cm thick. The upper left shows those measured on 7 November 2004, when the soil surface was not frozen. Measurements of sensible and latent heat fluxes made by the Bowen ratio method, H(B) and λE(B), agreed fairly well with those by the aerodynamic method, H(A) and λE(A). The upper right of the figure shows those measured on 9 December 2004, when the soil surface was frozen. The degree of agreement between the measurements of λE made by the two methods were also good.

The lower left of Figure 4 shows the diurnal variations in the energy balance terms measured on 26 November 2004, when unfrozen water content was decreasing at the 10–cm and 20–cm depths (Fig. 2). The sensible heat flux measured by the aerodynamic method was larger than the net radiation from midnight to early in the morning, which suggests that $Lf<0$ or heat was emitted from the soil surface layer. The heat flux measured by the Bowen ratio method assuming $Lf=0$ was a little bit smaller than that by the aerodynamic method, which also suggests that $Lf<0$ (Eq. 2). The lower right of the figure shows the variations on 23 March 2005, the last day of the period in which the soil at the 10–cm depth repeated thawing and freezing (Fig. 2). The latent heat flux measured by the Bowen ratio method assuming $Lf=0$ was a little bit larger than that by the aerodynamic method, which suggests that $Lf>0$ or heat of fusion was absorbed into the surface soil layer during the daytime.

It appears from the results shown above that, though the Bowen ratio method is impractical for measuring the evaporation from a frozen soil surface as was indicated by McKay and Thurtell (1978), the aerodynamic method can be used to measure the evaporation under freezing winter conditions. Table 4 shows daily evaporations measured by the aerodynamic method in the period when the surface soil layer 10 cm thick was frozen (23 November 2004 – 23 March 2005), which were obtained by integrating the evaporation rates measured on the hour or those interpolated from the measurements made before and after the time. In this period, daily mean evaporation is estimated to be about $0.5\,\mathrm{mm\,day^{-1}}$ and the cumulative evaporation for the period is estimated to be about 60 mm.

CONCLUDING REMARKS

Evaporation from a frozen soil surface was measured by the aerodynamic method, using a dimensionless stability function deduced by Webb (1970). This method is better than the Bowen ratio method when the evaporation from soil with a frozen surface is measured,

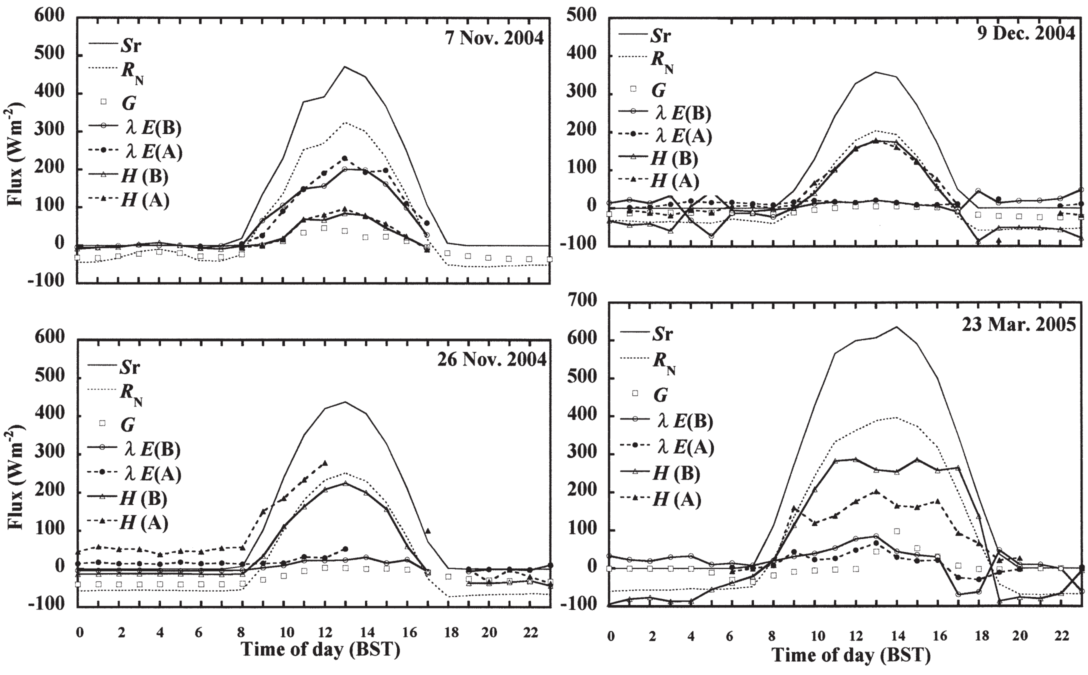

Fig. 4. Diurnal changes in the latent and sensible heat fluxes measured by the aerodynamic method, which are designated by (A), and those by the Bowen ratio method, which are designated by (B), for typical four days.

Table 4. Daily evaporations measured by the aerodynamic method. Insolations and daily maximum air temperatures are also given for reference

Date	Insolation (MJ)	Max air temp. (˚C)	Evap. (mmd^{-1})	Date	Insolation (MJ)	Max air temp. (˚C)	Evap. (mmd^{-1})
26 Nov.	9.3	–1.0	0.60	3 Feb.	7.0	–3.8	0.60
3 Dec.	6.4	3.1	0.84	18 Feb.	14.3	–13.2	0.27
6 Dec.	8.1	0.5	0.46	19 Feb.	14.3	–11.7	0.29
7 Dec.	8.0	2.8	0.32	3 Mar.	10.7	–4.2	0.56
9 Dec.	7.0	2.0	0.40	9 Mar.	14.1	13.7	1.29
26 Dec.	7.6	–9.8	0.17	16 Mar.	15.3	6.9	0.40
30 Dec.	8.3	–14.3	0.09	17 Mar.	12.7	–1.0	0.12
23 Jan. 05	8.9	–3.6	0.90	23 Mar.	17.6	5.1	0.30

because the latter requires estimating the heat flux equivalent to fusion or sublimation involved in the energy budget of the surface soil layer. However, it is difficult to make it in the field.

When the ground surface was frozen, latent heat flux was one order of magnitude smaller than sensible heat flux in the daytime and cumulative evaporation for the period in the experimental field irrigated late in autumn was estimated to be about 60 mm, which corresponds to about 25% of the amount of irrigation water (Kaneko *et al.*, submitted).

ACKNOWLEDGEMENTS

This research has been supported by the Core research for Evolutional Science and Technology (CREST) program of Japan Science and Technology Agency (JST). The authors would like to appreciate their grant in aid on this research. They also wish to thank Prof. T. Maki and Prof. T. Kusuda of Kyushu University for their encouragement.

REFERENCES

Kaneko, T., Kobayashi, T., Wang, W., He. W. and Cho, H. An evaluation of the overwinter loss of the water irrigated in late autumn in the upper reach of the Yellow River. *J. Japan Soc. Hydrol. & Water Resour.* **19**: (in press)

McKay, D. C. and Thurtell, G. W. 1978 Measurements of the energy fluxes involved in the energy budget of a snow cover. *J. Appl. Meteorol.*, **17**: 339–349

Monteith, J. L. and Unsworth, M. H., 1990 *Principles of Environmental Physics.*, 2nd ed., Edward Arnold, 1–291

Stein, J. and Kane, D., 1983 Monitoring the unfrozen water content of soil and snow using Time Domain Reflectometry. *Water Resour. Res.*, **19**: 1573–1584

Wang, L. and Akae, T., 2003 estimation of liquid water content by TDR measurements in frozen soils. *Trans. of JSIDRE*, **224**: 89–95

Wang, L. and Akae, T., 2004 Analysis of ground freezing process by unfrozen water content obtained from TDR data in Hetao Irrigation District of China. *J. Japan. Soc. Soil Phys.*, 11–19

Wang, W., Watanabe, E., Kobayashi, T., Cho, H., He, W. and Mohri, N., 2005 A method for measuring soil solution electrical conductivity in the field using TDR. *J. Japan Soc. Hydrol. & Water Resour.*, **18**: 55–63

Webb, E. K., 1970 Profile relationships: the log–linear range, and extension to strong stability. *Quart.J.Roy. Meteorol. Soc.*, **96**: 67–90